

Gauss-Bonnet Holographic Superconductors

Luke Barclay^{*}, Ruth Gregory[†], Sugumi Kanno[‡], Paul Sutcliffe[§]

*Centre for Particle Theory, Department of Mathematical Sciences
Durham University, South Road, Durham, DH1 3LE, UK*

ABSTRACT: We study holographic superconductors in five dimensional Einstein-Gauss-Bonnet gravity both numerically and analytically. We find the critical temperature of the superconductor decreases as backreaction is increased, although the effect of the Gauss-Bonnet coupling is more subtle: the critical temperature first decreases then increases as the coupling tends towards the Chern-Simons value in a backreaction dependent fashion. We compute the conductivity of the system, finding the energy gap, and show that the effect of both backreaction and higher curvature is to increase the gap ratio ω_g/T_c , thus there is no universal relation for these superconductors.

KEYWORDS: ads/cft, holography.

^{*}Email: luke.barclay@durham.ac.uk

[†]Email: r.a.w.gregory@durham.ac.uk

[‡]Email: sugumi.kanno@durham.ac.uk

[§]Email: p.m.sutcliffe@durham.ac.uk

Contents

1. Introduction	1
2. The Gauss-Bonnet bulk superconductor	3
3. Backreacting superconductors	7
4. Conductivity	9
5. Conclusion	13
A. Holographic renormalization	14

1. Introduction

The gauge gravity correspondence, [1], provides a fascinating tool to explore strongly coupled field theory. Recently, it has been applied to condensed matter systems yielding interesting qualitative results for systems exhibiting a superconducting phase [2]. In these, the bulk “classical” theory has gauge and charged scalar (or fermi) fields, and a black hole provides a finite temperature. Typically, no hair theorems, [3], would lead us to believe that the scalar field must be in its vacuum even in a highly charged black hole background, however, such theorems do not take account of the fact that in anti de Sitter spacetime scalar fields can have an apparently tachyonic mass, provided it is not too large, [4]; the confining properties of anti-de Sitter (adS) spacetime in essence prevent the instability from setting in unless the wavelength is sufficiently small. Once the scalar has a negative mode, the usual conditions of no-hair theorems cease to hold, and it becomes possible for the scalar to condense out of the vacuum in an analogous fashion to the condensation of SU(2) t’Hooft Polyakov fields outside a magnetic Reissner-Nordstrom solution [5].

The basic picture is that at a sufficiently low temperature, it becomes energetically feasible for a charged scalar to acquire an expectation value near the event horizon of the black hole, [6], spontaneously breaking the gauge symmetry and screening the charge and mass of the black hole. Because the asymptotic true vacuum is symmetric, the scalar has a power law fall-off near the boundary, and the coefficient of this fall-off can be interpreted as a condensate in the boundary theory. There is a reasonably complete understanding of these systems, including varying scalar mass

and potential, the gauge group, the number of spacetime dimensions, as well as having magnetic fields present and the stability of the system [6, 7, 8, 9, 10, 11, 12, 13]. While most of these models are “bottom up”, in the sense of being empirically constructed, similar models have been found from the top down perspective [14], and it is therefore of interest to consider more general stringy aspects of these models.

In a previous paper, some of us, [15], explored the stability of these empirical models to leading order corrections, by including on the gravitational side higher curvature terms, specifically, the Gauss-Bonnet (GB) invariant [16] which is believed to be the $\mathcal{O}(\alpha')$ correction to low energy string gravity [17]. We found that many of the qualitative features of the holographic superconductors were stable under higher curvature corrections, however, upon studying the conductivity, a more interesting story emerged. In [8], Horowitz and Roberts studied 2 and 3 + 1-dimensional holographic superconductors for a variety of bulk scalar masses. They discovered that the energy gap typically present in the real part of the conductivity, ω_g , was always about eight times as large as the critical temperature of the superconductor:

$$\omega_g \simeq 8T_c \tag{1.1}$$

this suggested that in spite of the different dimensions of the boundary condensate, there was some universal mechanism governing their superconductivity. Upon adding in higher curvature corrections however, this “universal” relation completely disappeared. This analysis was confirmed for more general models in [18], and although the expressions for conductivity used in these papers are not strictly accurate (see comments in section 4 and appendix A) the gap result is. The analyses presented in [15, 18] are however in the probe limit, i.e. where the matter fields do not backreact gravitationally on the spacetime, and since backreaction does typically alter the critical temperature, it is likely that a full computation will alter the relation between ω_g and T_c , potentially restoring the universal relation, at least for some value of the gravitational coupling for each α . In [19], the stability of the scalar condensate to higher curvature corrections was tested, and it was found that backreaction lowered T_c , as with Einstein gravity, thus making condensation harder. There was no qualitative difference however with the probe results.

In this paper we include the full effect of gravitational backreaction on the holographic superconductor with higher curvature terms. We find analytic bounds on the critical temperature, and cross-check these against exact results obtained by numerical computation. We then numerically compute the conductivity, and demonstrate that the conductivity does not in fact have a universal gap. Indeed, we find that even in Einstein gravity there is no universal gap once backreaction is taken into account. The organization of the paper is as follows: We first review the GB holographic superconductor in section 2, discussing the bulk model, clarifying possible ambiguities in the choice of mass of the scalar field and setting out some of the basic properties of

solutions to the system of equations. In section 3 we analyse the bulk equations analytically, providing bounds on the critical temperature and present numerical results for the condensation and critical temperature of the holographic superconductor. We then investigate the conductivity in section 4, first deriving the backreacted conductivity equation for GB gravity, then solving it numerically. Finally, we conclude in section 5.

2. The Gauss-Bonnet bulk superconductor

We begin with the Einstein-Gauss-Bonnet (EGB) gravitational action coupled to a massive charged complex scalar field and a U(1) gauge field:

$$S = \frac{1}{2\kappa^2} \int d^5x \sqrt{-g} \left[-R + \frac{12}{L^2} + \frac{\alpha}{2} (R^{abcd} R_{abcd} - 4R^{ab} R_{ab} + R^2) \right] + \int d^5x \sqrt{-g} \left[-\frac{1}{4} F^{ab} F_{ab} + |\nabla_a \psi - iq A_a \psi|^2 - m^2 |\psi|^2 \right] \quad (2.1)$$

where g is the determinant of the metric, and R_{abcd} , R_{ab} and R are the Riemann curvature tensor, Ricci tensor, and the Ricci scalar, respectively. We take the Gauss-Bonnet coupling constant α to be positive, and the negative cosmological constant term, $-6/L^2$, has been written in terms of a length scale, L . Note $\kappa^2 = 8\pi G_5$ gives an explicit Planck scale, and q is the charge, and m the mass, of the scalar field ψ ¹.

The equations of motion can be readily derived as:

$$R_{ab} - \frac{1}{2} R g_{ab} + \frac{6}{L^2} g_{ab} - \alpha \left[H_{ab} - \frac{1}{4} H g_{ab} \right] = 8\pi G T_{ab} \quad (2.2)$$

where

$$H_{ab} = R_a{}^{cde} R_{bcde} - 2R_{ac} R_b^c - 2R_{abcd} R^{cd} + R R_{ab} , \quad (2.3)$$

T_{ab} is the matter energy momentum tensor

$$T_{ab} = 2\mathcal{D}_{(a} \psi^\dagger \mathcal{D}_{b)} \psi - F_{ac} F_b{}^c - \left[|\mathcal{D}_c \psi|^2 - \frac{1}{4} F_{cd}^2 - m^2 |\psi|^2 \right] g_{ab} , \quad (2.4)$$

and $\mathcal{D}_a = \nabla_a - iq A_a$ is the gauge covariant derivative.

In the absence of any matter sources, the EGB equations have a pure adS solution

$$ds^2 = \frac{r^2}{L_e^2} \left[dt^2 - (dx^2 + dy^2 + dz^2) \right] - \frac{L_e^2}{r^2} dr^2 \quad (2.5)$$

with

$$L_e^2 = \frac{2\alpha}{1 - \sqrt{1 - \frac{4\alpha}{L^2}}} \rightarrow \begin{cases} L^2 , & \text{for } \alpha \rightarrow 0 \\ \frac{L^2}{2} , & \text{for } \alpha \rightarrow \frac{L^2}{4} \end{cases} . \quad (2.6)$$

¹Note that we follow Horowitz et al., [7], in taking a purely quadratic potential for the scalar field.

Thus the actual curvature of the adS spacetime is renormalized away from the cosmological constant scale, L , once α is nonzero. Since $L_e < L$, one could interpret switching α on as strengthening gravity, in the sense that a shorter lengthscale corresponds to stronger curvature.

To examine holographic superconductivity, we look for plane-symmetric black hole solutions with or without a nontrivial scalar, but with a nonzero charge. Taking the metric ansatz

$$ds^2 = f(r)e^{2\nu(r)}dt^2 - \frac{dr^2}{f(r)} - \frac{r^2}{L_e^2}(dx^2 + dy^2 + dz^2) \quad (2.7)$$

in the absence of a scalar field there is an analytic charged black hole solution, [20], with $\nu = 0$, and

$$A = \phi(r)dt = \frac{Q}{r_+^2} \left(1 - \frac{r_+^2}{r^2}\right) dt \quad (2.8)$$

$$f(r) = \frac{r^2}{2\alpha} \left[1 - \sqrt{1 - \frac{4\alpha}{L^2} \left(1 - \frac{r_+^4}{r^4}\right) + \frac{8\alpha\kappa^2 Q^2}{3r_+^4 r_+^2} \left(1 - \frac{r_+^2}{r^2}\right)} \right] \quad (2.9)$$

where Q is the charge of the black hole (up to a geometrical factor of 4π), and r_+ is the event horizon, which determines the ‘‘ADM’’ mass of the black hole [21]. In order to avoid a naked singularity, we need to restrict the parameter range as $\alpha \leq L^2/4$. Note that in the Einstein limit ($\alpha \rightarrow 0$), the solution (2.9) goes to the Reissner-Nordström adS black hole:

$$f(r) = \frac{r_+^2}{L^2} \left(\frac{r^2}{r_+^2} - \frac{r_+^2}{r^2}\right) + \frac{2\kappa^2 Q^2}{3r_+^4} \left(\frac{r_+^4}{r^4} - \frac{r_+^2}{r^2}\right). \quad (2.10)$$

In the Chern-Simons limit, $\alpha = L^2/4$, (so called because in odd dimensions the gravitational lagrangian becomes the potential for the Euler density in one dimension up, see e.g. [22]) the Newtonian potential takes the simpler form:

$$f(r) = \frac{2r^2}{L^2} - \frac{2r_+^2}{L^2} \sqrt{1 + 2L^2 \frac{\kappa^2 Q^2}{3r_+^6} \left(1 - \frac{r_+^2}{r^2}\right)}. \quad (2.11)$$

The superconducting phase corresponds to a ‘‘hairy’’ black hole, where the scalar field has condensed out of its symmetric state and screens the charge of the black hole. We can see that this will happen at sufficiently low temperature from Gubser’s rough argument, [6], using the scalar ‘effective mass’ $m_{\text{eff}}^2 = m^2 - q^2\phi(r)^2/f(r)$. For low temperature black holes, $f(r)$ increases slowly away from the horizon, giving a large negative mass squared over a sufficient range for an instability to set in. This is of course confirmed by the numerical results.

For the purposes of our investigation, we wish to have a fixed mass in order to focus on the effects of backreaction and the higher curvature terms. In [7], the

mass of the scalar was given in terms of the adS lengthscale ($m^2 = -(D - 2)/L^2$ in D -dimensions), and thus fixed with respect to the cosmological constant via the Einstein equations. In [15, 19] this same value of the mass was also chosen with respect to the *cosmological constant* scale L . However, in EGB gravity, the adS lengthscale is dependent on both L and α via (2.6), and fixing the mass with respect to L and not L_e means that the dimension of the operator in the dual boundary theory varies with α . It is possible therefore that some of the phenomena observed in [15, 19] are a consequence of this varying dimension, rather than intrinsic to the system, and we therefore fix the mass relative to the asymptotic adS lengthscale, $m^2 = -3/L_e^2$, in order that the boundary operator has fixed dimension 3.

In order to look for the hairy black hole solution, we take the standard static ansatz for the fields:

$$A_a = \phi(r)\delta_a^0, \quad \psi = \psi(r), \quad (2.12)$$

where without loss of generality ψ can be taken to be real. The full system of gravity and gauge-scalar equations of motion is then obtained as²:

$$\phi'' + \left(\frac{3}{r} - \nu'\right)\phi' - 2q^2\frac{\psi^2}{f}\phi = 0, \quad (2.13)$$

$$\psi'' + \left(\frac{3}{r} + \nu' + \frac{f'}{f}\right)\psi' + \left(\frac{q^2\phi^2}{f^2e^{2\nu}} - \frac{m^2}{f}\right)\psi = 0, \quad (2.14)$$

$$\left(1 - \frac{2\alpha f}{r^2}\right)\nu' = \frac{2\kappa^2}{3}r\left(\psi'^2 + \frac{q^2\phi^2\psi^2}{f^2e^{2\nu}}\right) \quad (2.15)$$

$$\left(1 - \frac{2\alpha f}{r^2}\right)f' + \frac{2}{r}f - \frac{4r}{L^2} = -\frac{2\kappa^2}{3}r\left[\frac{\phi'^2}{2e^{2\nu}} + m^2\psi^2 + f\psi'^2 + \frac{q^2\phi^2\psi^2}{fe^{2\nu}}\right] \quad (2.16)$$

where a prime denotes derivative with respect to r . These equations have several scaling symmetries, similar to those noted in [7], although as we have explicitly kept the Planck scale, an additional symmetry corresponding to a rescaling of energy is present.

1. $r \rightarrow ar, t, x^i \rightarrow at, ax^i, L \rightarrow aL, q \rightarrow q/a, \alpha \rightarrow a^2\alpha, A \rightarrow aA$.
2. $r \rightarrow br, t \rightarrow t/b, x^i \rightarrow x^i/b, f \rightarrow b^2f, \phi \rightarrow b\phi$.
3. $\phi \rightarrow c\phi, \psi \rightarrow c\psi, q \rightarrow q/c, \kappa^2 \rightarrow \kappa^2/c^2$.

We use these rescalings to set $L = Q = q = 1$ for numerical convenience. Note that in [7], the Planck scale was set to unity a priori, hence the probe limit corresponded to $q \rightarrow \infty$, as can be seen from the third rescaling. Also in contrast to [7], we choose

²Note, the ij component of the EGB equations is not independent via a Bianchi identity.

to fix $Q = 1$, so that we are explicitly holding the charge parameter fixed in all our computations.

Finally, the Hawking temperature is given by

$$T = \frac{1}{4\pi} f'(r) e^{\nu(r)} \Big|_{r=r_+}, \quad (2.17)$$

this will be interpreted as the temperature of the conformal field theory (CFT).

In order to solve our equations we need to impose boundary conditions at the horizon and the adS boundary.

- Horizon:

The position of the horizon, r_+ , is defined by $f(r_+) = 0$. Demanding regularity of the matter fields and metric at the horizon gives:

$$\phi(r_+) = 0, \quad \psi'(r_+) = \frac{m^2}{f'(r_+)} \psi(r_+). \quad (2.18)$$

Then equations (2.15) and (2.16) give:

$$\nu'(r_+) = \frac{2\kappa^2}{3} r_+ \left(\psi'(r_+)^2 + \frac{\phi'(r_+)^2 \psi(r_+)^2}{f'(r_+)^2 e^{2\nu(r_+)}} \right) \quad (2.19)$$

$$f'(r_+) = \frac{4}{L^2} r_+ - \frac{2\kappa^2}{3} r_+ \left(\frac{\phi'(r_+)^2}{2e^{2\nu(r_+)}} + m^2 \psi(r_+)^2 \right) \quad (2.20)$$

- Boundary:

As we want the spacetime to asymptote to adS in standard coordinates, we look for a solution with

$$\nu \rightarrow 0 \quad , \quad f(r) \sim \frac{r^2}{L_e^2} \quad \text{as } r \rightarrow \infty. \quad (2.21)$$

Asymptotically the solutions of ϕ and ψ are then found to be:

$$\phi(r) \sim P - \frac{Q}{r^2}, \quad \psi(r) \sim \frac{C_-}{r^{\Delta_-}} + \frac{C_+}{r^{\Delta_+}}, \quad (2.22)$$

where $\Delta_{\pm} = 2 \pm \sqrt{4 + m^2 L_e^2}$ for a general mass m^2 . In order to have a normalizable solution we take $C_- = 0$; P and C_+ are then fixed by consistency with the near horizon solution. According to the adS/CFT correspondence, we can interpret $\langle \mathcal{O}_{\Delta_+} \rangle \equiv C_+$, where \mathcal{O}_{Δ_+} is the operator with the conformal dimension Δ_+ dual to the scalar field. As already mentioned, we want the dimension of the boundary operator to remain fixed as we vary α and so we take $m^2 = -3/L_e^2$. Thus $\Delta_+ = 3$ for our choice of mass, and we compute the solutions of (2.13–2.16) numerically, reading off the r^{-3} fall-off of the scalar field to obtain $\langle \mathcal{O}_3 \rangle$ for a range of different temperatures.

3. Backreacting superconductors

As shown in [15], the scalar field condenses out of its vacuum near the horizon of a sufficiently small black hole. Although the mass chosen for the scalar in [15] is different to that used here ($m'^2 = -3/L^2 \geq -3/L_e^2$) we still expect a similar qualitative behaviour. Thus, in computing the dependence of $\langle \mathcal{O}_3 \rangle$ with T , we expect to see the characteristic curve depicting the condensation of $\langle \mathcal{O}_3 \rangle$ from being trivially zero above some critical temperature T_c , to some nonzero value below this critical temperature. Before proceeding with a full numerical analysis, it is useful to obtain some analytic understanding of the phase transition and the critical temperature.

In order to find analytic bounds for the critical temperature, we look at the scalar field equation near T_c . For temperatures just below T_c , the scalar is only marginally away from its vacuum, hence the metric and gauge field will have the form (2.8, 2.9), up to corrections of order $\mathcal{O}(\psi^2)$, thus the scalar field satisfies a linear equation (2.14) with f and ϕ taking their background values.

A crude upper bound for T_c can be found by considering the variable $X = r^2\psi$, which satisfies to leading order:

$$X'' + \left(\frac{f'_0}{f_0} - \frac{1}{r} \right) X' + \left(\frac{q^2\phi^2}{f_0^2} + \frac{3}{L_e^2 f_0} - \frac{2f'_0}{r f_0} \right) X = 0. \quad (3.1)$$

At the horizon,

$$X'(r_+) = \frac{X(r_+)}{4\pi T_c} \left(\frac{8}{L^2} - \frac{3}{L_e^2} - \frac{8\kappa^2 Q^2}{3r_+^6} \right) \quad (3.2)$$

which is positive for small $\kappa^2 Q^2$ (taking $X(r_+) > 0$ without loss of generality). Since $X \sim 1/r$ as $r \rightarrow \infty$, the solution must have a maximum for some r , which requires that

$$\left(\frac{q^2\phi^2}{f_0^2} + \frac{3}{L_e^2 f_0} - \frac{2f'_0}{r f_0} \right) > 0 \quad (3.3)$$

at this point. An examination of when this condition is violated provides an upper bound for T_c . This bound is only reliable for weakly gravitating systems, and figure 1 shows the upper bound for no backreaction, and $\kappa^2 = 0.05$. For larger values of κ^2 , the method fails because the behaviour of the function in (3.3) qualitatively changes.

In order to obtain a lower bound, consider instead $Y = rX$, then manipulating the equation of motion for Y implies that *if* a solution exists, then the integral

$$\int_{r_+}^{\infty} \frac{1}{r^3} \left[\frac{\phi_0^2}{f_0} + \frac{3}{L_e^2} + \frac{3f_0}{r^2} - \frac{3f'_0}{r} \right] = - \int_{r_+}^{\infty} \frac{f_0 Y'^2}{r^3 Y^2} \leq 0 \quad (3.4)$$

is negative. Note that negativity of this integral does not imply existence of a solution to the linearized equation near T_c , it is simply a necessary condition. Since this integral is always negative at large T , and positive as $T \rightarrow 0$ (for $\kappa^2 \lesssim 0.4$), observing where it changes sign provides a lower bound on T_c . This bound gives an extremely

reliable indicator of T_c for a good range of κ^2 , well within the numerical range we were able to explore.

The analytic bounds for T_c have been plotted in figure 1 together with the exact values of T_c obtained by numerical computation. The upper bound has only been shown for $\kappa^2 \leq 0.05$, as above this value it becomes less predictive and clutters the plot, and indeed beyond $\kappa^2 \sim 0.2$ (corresponding to $q \sim 2.25$ in the notation of [7]) it ceases to have quantitative value for any α . The lower bound on the other hand becomes successively more accurate as the values of κ^2 are stepped up, and gives a very good quantitative guide to the behaviour of T_c as we vary α and κ^2 .

It is easy to see that the effect of backreaction is to decrease T_c and thus make condensation harder. We can see this from the point of view of the bounds, as backreaction at fixed Q drops the temperature of the black hole and also gives a smoother profile for f_0 , which makes it harder for the bound (3.4) to be satisfied. Essentially, the effect of backreaction is that the condensation of the scalar field not only screens the charge of the black hole, but also its mass, as the scalar and gauge fields now contribute to the ADM mass. This means that for a given charge and temperature, the radius of the black hole is increased, which makes it harder for the scalar to condense.

One very interesting feature clearly exhibited in the bounds is the turning point in T_c as a function of α for fixed κ^2 . In the probe case, this occurs very near the Chern-Simons limit $\alpha = L^2/4$, and is barely perceptible in the numerical data, however this is shown clearly in the upper bound in particular. (We checked the numerical data by taking very small steps in the α parameter near $L^2/4$, and were able to confirm this feature in the numerical data, however, these points are not shown for clarity.) Once backreaction is switched on, the minimum becomes much more pronounced, and indeed for large backreaction ($\kappa^2 = 0.2$) the Chern-Simons limit is showing a considerable enhancement of T_c over the typical values for lower α .

In order to find the actual behaviour of the bulk superconductor, we integrated (2.13–2.16) numerically. As already stated, we took $L = Q = q = 1$, and varied r_+ to study how the system reacted to varying temperature. After solving for the matter and gravitational fields, the temperature is computed and the value of $\langle \mathcal{O}_3 \rangle$ read off.

Figure 2 shows $\langle \mathcal{O}_3 \rangle^{1/3}$ as a function of temperature for a variety of values of α and κ^2 . Each line in the plot forms the characteristic curve of $\langle \mathcal{O}_3 \rangle^{1/3}$ condensing at some critical temperature. For simplicity we chose three values of α to display the features of the system: the Einstein limit ($\alpha = 0$), the Chern-Simons limit ($\alpha = 0.25$), and the mid-point value $\alpha = 0.125$ to represent a ‘generic’ value of α . We also only present the detailed information for two values of κ^2 : the case of no backreaction ($\kappa^2 = 0$), and a backreaction of $\kappa^2 = 0.1$. The plots are qualitatively similar for other values of κ^2 and α , and can be deduced from the information in figure 1 on critical temperature.

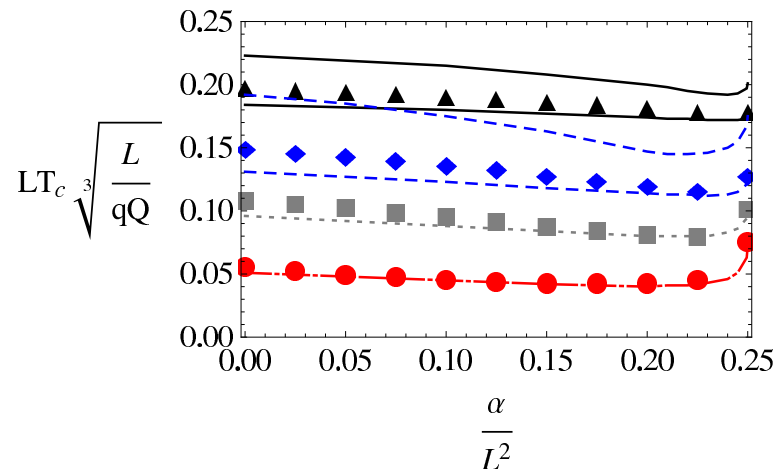


Figure 1: A plot of the critical temperature as a function of α for a selection of κ^2 . The analytic bounds are shown as lines and the numerical data as points. Respectively: $\kappa^2 = 0$ is shown in black, with solid lines and triangular data points; $\kappa^2 = 0.05$ has blue dashed lines and diamonds; $\kappa^2 = 0.1$ has a grey dotted line and squares; $\kappa^2 = 0.2$ has a red dot-dash line with circular data points. The lower bound is shown for all κ^2 values, but the upper bound is shown only for the lowest two values of κ^2 , as they overlap significantly with the other data and confuse the plot.

Figure 2(a), which displays the raw data, shows how varying α and κ^2 effects the height, shape and critical temperature of the condensate. This gives an alternate visualisation to figure 1 of the effect of both backreaction and higher curvature terms on the critical temperature. Note how the backreacting case clearly exhibits the special nature of the Chern-Simons limit. Note also the disparity in the unnormalized condensate value. As in figure 1, we see that increasing κ^2 reduces the critical temperature of the system markedly. We also see the effect of α , which initially lowers T_c , then increases it again for α approaching the Chern-Simons limit. Because we are only showing the data for three values of α , the non-backreacting data do not display this effect, but it is clearly present in the backreacting data, and indeed increasing κ^2 enhances this effect,

Figure 2(b) shows the curves normalized by T_c . The effect of κ^2 is to increase the height of these graphs, in spite of the fact that the raw data tends to have lower values of $\langle \mathcal{O}_3 \rangle$. This is clearly because the most significant impact of increasing gravitational backreaction is that the critical temperature of the system is lowered. In this case the effect of backreaction is extremely marked, with the condensate varying more widely with α .

4. Conductivity

In [8], Horowitz and Roberts observed an interesting phenomenon for the conductiv-

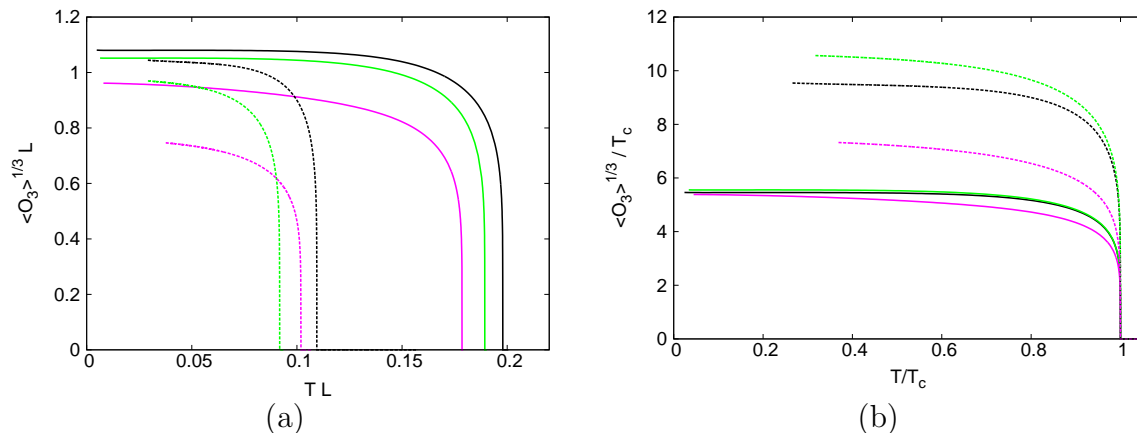


Figure 2: Two plots of the condensate as a function of temperature for a selection of values of α and κ^2 . In each case, solid lines correspond to $\kappa^2 = 0$ and dotted lines to $\kappa^2 = 0.1$. The black plot is $\alpha = 0$, green is $\alpha = 0.125$ and magenta is $\alpha = 0.25$. The first plot shows unnormalized data, which indicates the variation of critical temperature as both α and κ^2 vary. Plot (b) shows the conventional plot of condensate against temperature, both rendered dimensionless by normalizing to T_c .

ity of the boundary theory. They considered the model (2.1) in the probe Einstein limit for a range of different bulk scalar masses, and on computing the conductivity found an apparent universal relation

$$\frac{\omega_g}{T_c} \simeq 8, \quad (4.1)$$

with deviations of less than 8 %. In [15] we found evidence that this “universality” was not in fact stable to the presence of stringy corrections, and we now wish to test the robustness of this result to backreaction.

Conductivity is conventionally expressed as the current density response to an applied electric field:

$$\sigma = \frac{\mathcal{J}}{\mathcal{E}}. \quad (4.2)$$

As the bulk field A_μ corresponds to a boundary four-current J_μ we must examine perturbations of A_μ to compute the conductivity. Since we are dealing with full gravitational backreaction, we must also perturb the metric, and compute the variation of the EGB gravity equations. After some algebra we find:

$$\dot{h}'_{ti} - \frac{2}{r}\dot{h}_{ti} - \ddot{h}_{ri} + \frac{L^2 f e^{2\nu}}{r^2 - 2\alpha f} \left(1 - \frac{\alpha(2\nu' f + f')}{r} \right) \Delta h_{ri} + \frac{2\kappa^2 r^2 \dot{A}_i \phi'}{r^2 - 2\alpha f} = 0 \quad (4.3)$$

$$\frac{e^{-\nu}}{r f} [r f e^\nu A'_i]' - \frac{\ddot{A}_i}{f^2 e^{2\nu}} + \frac{L^2}{r^2 f} \Delta A_i - \frac{2}{f} q^2 \psi^2 A_i + \frac{\phi'}{f e^{2\nu}} \left(h'_{ti} - \frac{2}{r} h_{ti} - \dot{h}_{ri} \right) = 0 \quad (4.4)$$

where h_{ab} is the perturbation of the metric tensor, and A_i is the perturbation of the gauge field, which has only spatial components. Writing $A_i(t, r, x^i) = A(r) e^{i\mathbf{k}\cdot\mathbf{x} - i\omega t} e_i$,

and setting $\mathbf{k} = \mathbf{0}$, we can integrate (4.3), and substitute in (4.4) to obtain:

$$A'' + \left(\frac{f'}{f} + \nu' + \frac{1}{r} \right) A' + \left[\frac{\omega^2}{f^2 e^{2\nu}} - \frac{2}{f} q^2 \psi^2 - \frac{2\kappa^2 r^2 \phi'^2}{f e^{2\nu} (r^2 - 2\alpha f)} \right] A = 0 . \quad (4.5)$$

We solve this under the physically imposed boundary condition of no outgoing radiation at the horizon:

$$A(r) \sim f(r)^{-i\frac{\omega}{4\pi T_+}} . \quad (4.6)$$

Here, T_+ is the Hawking temperature defined at $r = r_+$. In the asymptotic adS region ($r \rightarrow \infty$), the general solution takes the form

$$A = a_0 + \frac{a_2}{r^2} + \frac{a_0 L_e^4 \omega^2}{2r^2} \log \frac{r}{L} \quad (4.7)$$

where a_0 and a_2 are integration constants. Note there is an arbitrariness of scale in the logarithmic term, as pointed out in [8], however, this is related to an arbitrariness in the holographic renormalization process (see Appendix A) and we present here the expression used in our numerical computations to extract the behaviour of the gauge field.

To calculate the conductivity, we must therefore compute the current dual to the gauge field (4.7), and its linear response to an applied electric field. Since the details of the correspondence are α dependent (the asymptotic adS lengthscale changes with α), we go through the explicit calculation in an appendix. The result of this computation is³

$$\sigma = \frac{2a_2}{i\omega L_e^4 a_0} + \frac{i\omega}{2} - i\omega \log \left(\frac{L_e}{L} \right) . \quad (4.8)$$

Note that the imaginary term linear in ω has an arbitrariness of scale from the counterterm subtraction, and in practise when we present the plots of ω we will make use of this fact to choose an appropriate renormalization scale to give the greatest transparency of the features inherent in the conductivity.

Figures 3 and 4 present various aspects of our results for the conductivity at a range of values of α and κ^2 . In figure 3 we show the real and imaginary parts of the conductivity as a function of ω/T_c for no backreaction and a backreaction of $\kappa^2 = 0.05$ for our three sample values of α : 0, 0.125, and 0.25.

In each of these plots, the gap is clearly indicated by a rise in the real part of σ , which coincides with the global minimum of $\text{Im}(\sigma)$. As was noted in the derivation of (4.8), the imaginary part is only valid up to a linear term in ω , the size of which is dependent on the renormalization scheme employed (and also on the charge Q). Certainly, within the parameter range tested, one can always find an appropriate term to create a finite global minimum in $\text{Im}(\sigma)$ if it is not initially present. As

³Note that the equation for conductivity in [15] was missing some factors of L_e : (4.7) and (4.8) correct equations (4.4) and (4.7) there.

in [8], we suggest that the value of this minimum be taken as ω_g , the value of the frequency gap. This has a clear advantage over trying to determine the midpoint of the step in $\text{Re}(\sigma)$, in that it gives an unambiguous value of ω_g . As the plots clearly show, once backreaction is included, the ‘step’ becomes much more gentle and extended, and while the dip in $\text{Im}(\sigma)$ is smoothed, it is still clearly apparent, even for the most extreme, backreacting Chern-Simons, case.

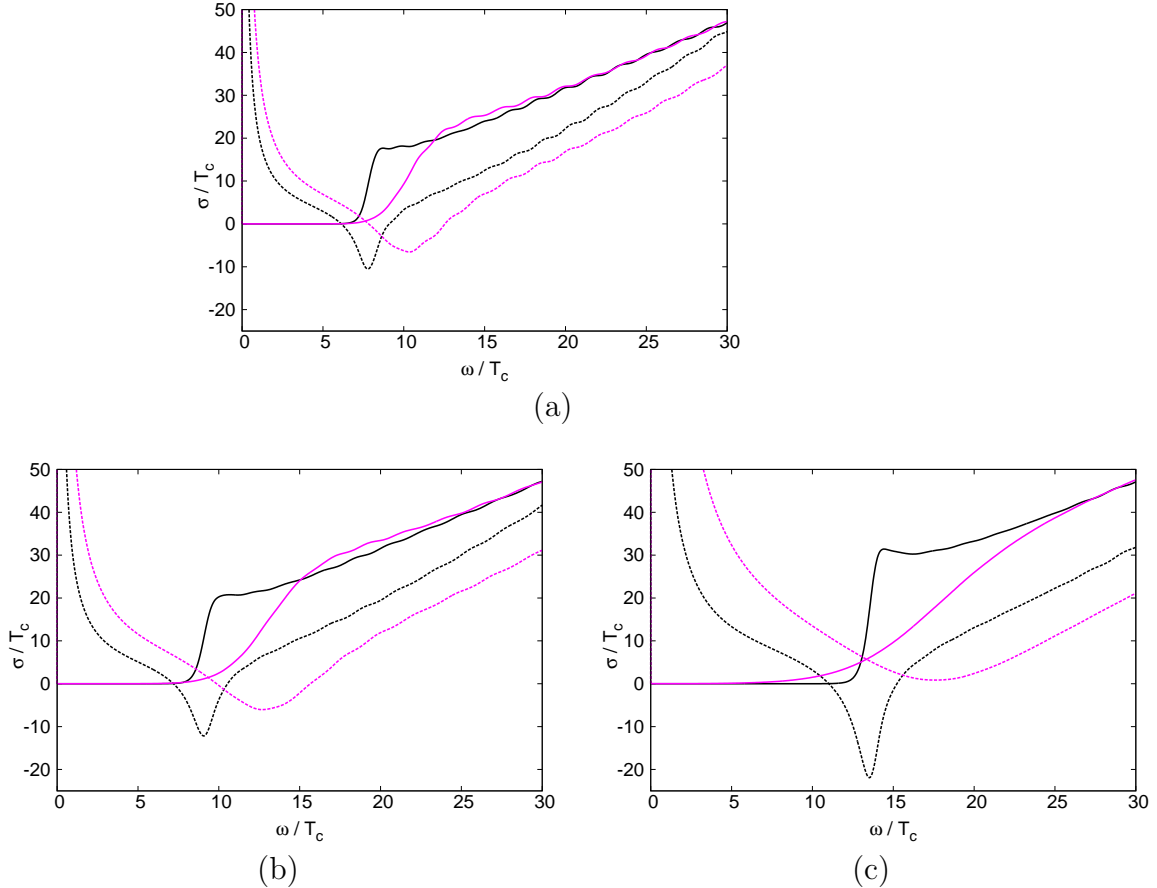


Figure 3: Conductivity: a range of plots showing the real (solid line) and imaginary (dashed line) parts of the conductivity as a function of frequency. Both variables are normalized by T_c to dimensionless parameters. In each case the conductivity is shown for no backreaction in black, and for a backreacting parameter $\kappa^2 = 0.05$ in magenta. Each plot represents a different representative value of α : (a) is $\alpha = 0$, (b) is $\alpha = 0.125$, and (c) is $\alpha = 0.25$. The slight undulations in the plots at large ω is a numerical artefact due to the sensitivity of the system near the horizon.

The frequency gap is a distinct characteristic of a superconductor and in the BCS theory of superconductivity this frequency gap corresponds to the minimum energy required to break a Cooper pair. As mentioned above, in [8] it was claimed that for the holographic superconductor the relation $\omega_g/T_c \simeq 8$ had a certain universality, proving stable for a range of scalar masses and dimensions. In [15] this

relation was shown to be unstable to Gauss-Bonnet corrections in the probe limit (for $m^2 = -3/L^2$), and we unequivocally confirm this feature. Figure 4 gives a very clear indicator of how backreaction and higher curvature terms affect the gap. Increasing either α or κ^2 increases ω_g/T_c . For the case of increasing α , the effect occurs mainly because of a shift in the gap, rather than a significant alteration of T_c , which varies much more strongly with backreaction than α . On the other hand, varying κ^2 practically does not alter ω_g at all, whereas T_c drops dramatically, leading to a sharp rise in ω_g/T_c .

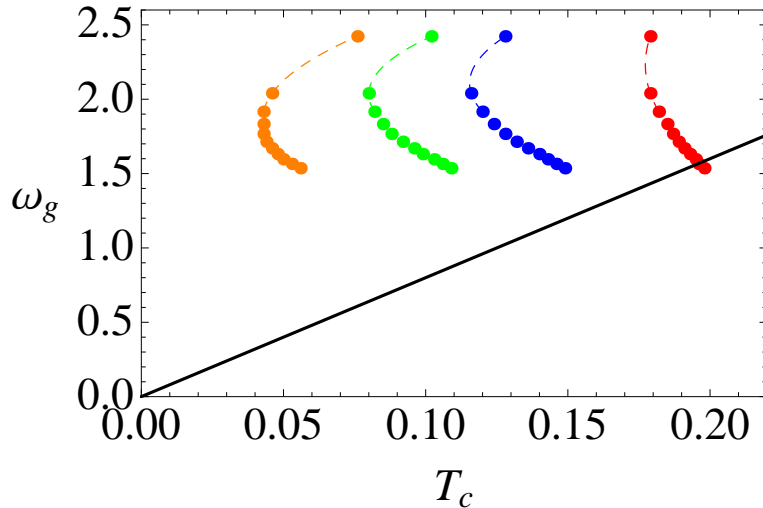


Figure 4: The gap frequency as a function of T_c (the line $\omega_g = 8T_c$ is shown in black). Each data point on the graph represents a single pair (α, κ^2) . The different colours represent different degrees of backreaction; from right to left: Red is $\kappa^2 = 0$, Blue is $\kappa^2 = 0.05$, Green 0.1, and Orange $\kappa^2 = 0.2$. In each case α is incremented from 0 to 0.25. As the gap alters rapidly near the Chern-Simons limit, the dotted lines are added by hand to guide the eye.

5. Conclusion

The aim of this paper was to understand how including both Gauss-Bonnet corrections and backreaction might affect the holographic superconductor. Our results are clear: increasing backreaction lowers the critical temperature of the superconductor hence increasing ω_g/T_c . The effect of higher curvature terms is more subtle. Although these initially act in a similar fashion to backreaction in lowering the critical temperature, for significant GB coupling the critical temperature eventually begins to increase. The conductivity gap is also modified, with both ω_g and T_c altering to increase the ratio ω_g/T_c . We have therefore unambiguously refuted the claim that there is a universal gap $\omega_g \simeq 8T_c$ for these holographic superconductors, as even in the Einstein limit there is no such relation.

Our results show that there is a rich structure in higher dimensional holographic superconductors, with or without higher curvature corrections. For simplicity, we focussed on a single value of the scalar mass which fixed the dimension of the boundary operator. We believe this will clearly differentiate the effects of the backreaction and higher curvature coupling. From the results of [18] we do not expect any qualitative differences to appear from a varying mass, although there will undoubtedly be quantitative differences, particularly since the expressions for conductivity used are inaccurate (as can easily be seen from dimensional grounds). It would be useful to explore more fully this parameter space, and to see if altering the bulk potential further enhances the features of the system, as well as exploring nonabelian gauge fields and more complex superconductors.

Acknowledgments

We would like to thank Jiro Soda for previous collaboration and helpful input during this work. We would also like to thank Simon Ross and Misao Sasaki for useful conversations. LB is supported by an STFC studentship, RG, SK and PMS acknowledge the support of STFC under the rolling grant ST/G000433/1.

A. Holographic renormalization

In this, we follow the method of Skenderis [23] and explicitly compute the counterterm and current dual to the electromagnetic bulk perturbation. First, we choose coordinates so that⁴

$$ds^2 = h_{\mu\nu} d\xi^\mu d\xi^\nu - L_e^2 \frac{d\rho^2}{\rho^2} \quad (\text{A.1})$$

Clearly, asymptotically, $\rho = L_e^2/r^2 \rightarrow 0$, and $\xi^\mu = x^\mu/L_e$ with

$$ds^2 \sim L_e^2 \left[\frac{d\tau^2 - d\xi_i^2}{\rho} - \frac{d\rho^2}{\rho^2} \right] \quad (\text{A.2})$$

We then expand

$$h_{\mu\nu} = \frac{L_e^2}{\rho} [\gamma_{\mu\nu}^{(0)} + \rho^2 \gamma_{\mu\nu}^{(4)}] \quad (\text{A.3})$$

$$A_\mu = L_e^{-1/2} [A_\mu^{(0)} + \rho A_\mu^{(2)} + \dots] \quad (\text{A.4})$$

and solve the equations of motion order by order in ρ . (The factor of $L_e^{-1/2}$ ensures that the gauge fields $A_\mu^{(n)}$ have the correct dimensionality.)

⁴Note that the $h_{\mu\nu}$ here is distinct from the h_{ab} metric perturbation notation used in section 4!

Focussing on the electromagnetic contribution, we can evaluate the action on-shell:

$$\begin{aligned}
S &= \int_{\mathcal{M}} -\frac{1}{4} F_{ab}^2 \sqrt{g} d^5x \\
&= \int_{\mathcal{M}} \frac{1}{2} A_b \nabla_a F^{ab} \sqrt{g} d^5x - \int_{\partial\mathcal{M}} \frac{1}{2} F^{ab} n_a A_b \sqrt{h} d^4x \\
&= L_e \int_{\rho=\epsilon} A'_\mu A_\nu \gamma^{(0)\mu\nu} \sqrt{\gamma^{(0)}} d^4x
\end{aligned} \tag{A.5}$$

In these new coordinates, the gauge field equation of motion takes the form

$$\rho \frac{d^2 A_i}{d\rho^2} - \frac{1}{4} \partial_{(0)}^2 A_i = \mathcal{O}(\rho^2) \tag{A.6}$$

where $\partial_{(0)}^2$ represents the wave operator with respect to the boundary metric $\gamma_{\mu\nu}^{(0)}$. The solution to this equation is

$$A_i = L_e^{-1/2} A_i^{(0)} + \rho L_e^{-1/2} \left[A_i^{(2)} + \frac{1}{4} \ln \rho \partial_{(0)}^2 A_i^{(0)} \right] \tag{A.7}$$

Thus the on-shell action,

$$S = - \int_{\rho=\epsilon} A_i^{(0)} \left[A_i^{(2)} + \frac{1}{4} \partial_{(0)}^2 A_i^{(0)} + \frac{1}{4} \ln \epsilon \partial_{(0)}^2 A_i^{(0)} \right] \sqrt{\gamma^{(0)}} d^4x, \tag{A.8}$$

is logarithmically divergent. In order to find the correct counterterm, we must invert the series solution (A.7) to give $A_i^{(0)} = \sqrt{L_e} A_i + \mathcal{O}(\epsilon)$, and hence obtain:

$$\begin{aligned}
S_{ct} &= \frac{L_e}{4} \ln \epsilon \int_{\rho=\epsilon} A_i \partial_{(0)}^2 A_i \sqrt{\gamma^{(0)}} d^4x \\
&= \frac{L_e}{4} \ln \epsilon \int_{\rho=\epsilon} \frac{1}{2} F_{\mu\nu}^2 \sqrt{h} d^4x
\end{aligned} \tag{A.9}$$

We can now compute the boundary current, which is given by the 1-point function

$$\langle J^\mu \rangle = L_e^{-1/2} \frac{\delta S_{ren}}{\delta A_\mu} \tag{A.10}$$

Varying $S + S_{ct}$ explicitly gives

$$\begin{aligned}
\delta S + \delta S_{ct} &= \int_{\mathcal{M}} -F^{ab} \partial_a \delta A_b \sqrt{g} d^5x + \frac{L_e}{2} \ln \epsilon \int_{\rho=\epsilon} F^{\mu\nu} \partial_\mu \delta A_\nu \sqrt{h} d^4x \\
&= L_e \int_{\rho=\epsilon} \sqrt{\gamma^{(0)}} d^4x \delta A_i \left(-2A'_i + \frac{\ln \epsilon}{2} \partial_{(0)}^2 A_i \right)
\end{aligned} \tag{A.11}$$

Substituting for A_i from (A.7) gives

$$\begin{aligned}
L_e^{-1/2} \frac{\delta S_{ren}}{\delta A_i} &= -2 \left[A_i^{(2)} + \frac{1}{4} \ln \epsilon \partial_{(0)}^2 A_i^{(0)} + \frac{1}{4} \partial_{(0)}^2 A_i^{(0)} \right] + \frac{\ln \epsilon}{2} \partial_{(0)}^2 A_i^{(0)} \\
&= -2A_i^{(2)} - \frac{1}{2} \partial_{(0)}^2 A_i^{(0)} = -2A_i^{(2)} + \frac{\hat{\omega}^2 - \hat{\mathbf{k}}^2}{2} A_i^{(0)}
\end{aligned} \tag{A.12}$$

where the hatted quantities correspond to frequencies or wavenumbers with respect to the dimensionless coordinates ξ^i . Notice that a shift in the renormalization scale $\epsilon \rightarrow \lambda\epsilon$, results in a shift of the coefficient of the final term of $\ln \lambda/2$.

To get the conductivity, we can either compute the two-point function following [24], or use the standard formula (4.2), noting that $E = \dot{A}_i^{(0)}$, to get the dimensionless conductivity as

$$\hat{\sigma} = \left. \frac{2A^{(2)}}{i\omega A^{(0)}} \right|_{\mathbf{k}=0} + \frac{i\omega}{2} \quad (\text{A.13})$$

Finally, to obtain a dimensionally correct expression in terms of our original coordinates, we rewrite (A.7)

$$\begin{aligned} A_i &= L_e^{-1/2} A_i^{(0)} + \frac{L_e^{3/2}}{r^2} \left[A_i^{(2)} - \frac{1}{2} \ln \frac{r}{L_e} \partial_{(0)}^2 A_i^{(0)} \right] \\ &= L_e^{-1/2} \left[A_i^{(0)} + \frac{L_e^2}{r^2} \left(A_i^{(2)} + \ln\left(\frac{L_e}{L}\right) \frac{L_e^2(\mathbf{k}^2 - \omega^2)}{2} A_i^{(0)} \right) - \frac{L_e^4(\mathbf{k}^2 - \omega^2)}{2r^2} \ln\left(\frac{r}{L}\right) A_i^{(0)} \right] \end{aligned} \quad (\text{A.14})$$

from which we obtain

$$\sigma = \frac{2a_2}{i\omega L_e^4 a_0} - i\omega \ln\left(\frac{L_e}{L}\right) + \frac{i\omega}{2} \quad (\text{A.15})$$

This is now the dimensionally correct expression for the conductivity, although there is an ambiguity in the imaginary part of $i\omega \ln \lambda/2$ as already noted. This differs from the expressions in [15, 18] by factors of L_e , mainly due to an incorrect extrapolation of the relation $G^R = -rfAA'|_{r \rightarrow \infty}$ from the Einstein limit.

References

- [1] J. M. Maldacena, Adv. Theor. Math. Phys. **2**, 231 (1998) [Int. J. Theor. Phys. **38**, 1113 (1999)] [arXiv:hep-th/9711200].
- [2] C. P. Herzog, J. Phys. A **42**, 343001 (2009) [arXiv:0904.1975 [hep-th]].
S. A. Hartnoll, Class. Quant. Grav. **26**, 224002 (2009) [arXiv:0903.3246 [hep-th]].
G. T. Horowitz, “Introduction to Holographic Superconductors,” arXiv:1002.1722 [hep-th].
- [3] J. D. Bekenstein, “Black hole hair: Twenty-five years after,” arXiv:gr-qc/9605059.
T. Hertog, Phys. Rev. D **74**, 084008 (2006) [arXiv:gr-qc/0608075].
- [4] P. Breitenlohner and D. Z. Freedman, Annals Phys. **144**, 249 (1982).
- [5] K. M. Lee, V. P. Nair and E. J. Weinberg, Phys. Rev. Lett. **68**, 1100 (1992) [arXiv:hep-th/9111045].
K. M. Lee, V. P. Nair and E. J. Weinberg, Phys. Rev. D **45**, 2751 (1992) [arXiv:hep-th/9112008].

- [6] S. S. Gubser, *Class. Quant. Grav.* **22**, 5121 (2005) [arXiv:hep-th/0505189].
Phys. Rev. D **78**, 065034 (2008) [arXiv:0801.2977 [hep-th]].
- [7] S. A. Hartnoll, C. P. Herzog and G. T. Horowitz, *Phys. Rev. Lett.* **101**, 031601 (2008) [arXiv:0803.3295 [hep-th]].
S. A. Hartnoll, C. P. Herzog and G. T. Horowitz, *JHEP* **0812**, 015 (2008) [arXiv:0810.1563 [hep-th]].
- [8] G. T. Horowitz and M. M. Roberts, *Phys. Rev. D* **78**, 126008 (2008) [arXiv:0810.1077 [hep-th]].
- [9] S. S. Gubser and A. Nellore, *Phys. Rev. D* **80**, 105007 (2009) [arXiv:0908.1972 [hep-th]].
G. T. Horowitz and M. M. Roberts, *JHEP* **0911**, 015 (2009) [arXiv:0908.3677 [hep-th]].
R. A. Konoplya and A. Zhidenko, *Phys. Lett. B* **686**, 199 (2010) [arXiv:0909.2138 [hep-th]].
- [10] S. S. Gubser and S. S. Pufu, *JHEP* **0811**, 033 (2008) [arXiv:0805.2960 [hep-th]].
K. Peeters, J. Powell and M. Zamaklar, *JHEP* **0909**, 101 (2009) [arXiv:0907.1508 [hep-th]].
- [11] K. Maeda, M. Natsuume and T. Okamura, *Phys. Rev. D* **79**, 126004 (2009) [arXiv:0904.1914 [hep-th]].
- [12] E. Nakano and W. Y. Wen, *Phys. Rev. D* **78**, 046004 (2008) [arXiv:0804.3180 [hep-th]].
T. Albash and C. V. Johnson, *JHEP* **0809**, 121 (2008) [arXiv:0804.3466 [hep-th]].
- [13] T. Takahashi and J. Soda, *Phys. Rev. D* **79**, 104025 (2009) [arXiv:0902.2921 [gr-qc]].
S. Kanno and J. Soda, “Stability of Holographic Superconductors,” arXiv:1007.5002 [hep-th].
- [14] S. S. Gubser, C. P. Herzog, S. S. Pufu and T. Tesileanu, *Phys. Rev. Lett.* **103**, 141601 (2009) [arXiv:0907.3510 [hep-th]].
J. P. Gauntlett, J. Sonner and T. Wiseman, *Phys. Rev. Lett.* **103**, 151601 (2009) [arXiv:0907.3796 [hep-th]].
- [15] R. Gregory, S. Kanno and J. Soda, *JHEP* **0910**, 010 (2009) [arXiv:0907.3203 [hep-th]].
- [16] D. Lovelock, *J. Math. Phys.* **12**, 498 (1971).
- [17] D. J. Gross and J. H. Sloan, *Nucl. Phys. B* **291**, 41 (1987).
R. R. Metsaev and A. A. Tseytlin, *Nucl. Phys. B* **293**, 385 (1987).
- [18] Q. Pan, B. Wang, E. Papantonopoulos, J. Oliveira and A. B. Pavan, *Phys. Rev. D* **81**, 106007 (2010) [arXiv:0912.2475 [hep-th]].

- X. H. Ge, B. Wang, S. F. Wu and G. H. Yang, JHEP **1008**, 108 (2010) [arXiv:1002.4901 [hep-th]].
- Q. Pan and B. Wang, “General holographic superconductor models with Gauss-Bonnet corrections,” arXiv:1005.4743 [hep-th].
- R. G. Cai, Z. Y. Nie and H. Q. Zhang, “Holographic p-wave superconductors from Gauss-Bonnet gravity,” arXiv:1007.3321 [hep-th].
- [19] Y. Brihaye and B. Hartmann, Phys. Rev. D **81**, 126008 (2010) [arXiv:1003.5130 [hep-th]].
- [20] D. G. Boulware and S. Deser, Phys. Rev. Lett. **55**, 2656 (1985).
R. G. Cai, Phys. Rev. D **65**, 084014 (2002) [arXiv:hep-th/0109133].
- [21] L. F. Abbott and S. Deser, Nucl. Phys. B **195**, 76 (1982).
S. Deser and B. Tekin, Phys. Rev. D **67**, 084009 (2003) [arXiv:hep-th/0212292].
- [22] M. Banados, C. Teitelboim and J. Zanelli, Phys. Rev. D **49**, 975 (1994) [arXiv:gr-qc/9307033].
- [23] K. Skenderis, Class. Quant. Grav. **19**, 5849 (2002) [arXiv:hep-th/0209067].
- [24] D. T. Son and A. O. Starinets, JHEP **0209**, 042 (2002) [arXiv:hep-th/0205051].